Experimental study and analytical modeling of preferential flow and partitioning dynamics at unsaturated fracture intersections

Torsten Noffz[1], Marco Dentz[2], and Jannes Kordilla[1]

[1]University of Goettingen, Dept. of Applied Geology, Germany <tnoffz@gwdg.de>

[2]Institute of Environmental Assessment and Water Research (IDAEA), Spanish National Research Council (CSIC), Spain <marco.dentz@csic.es>

I. Introduction

1. Unsaturated flow

- Complex, gravity-driven flow dynamics in macropores of soils (Nimmo, 2012) and along fracture networks (Dahan et al. 1999, 2000; Kordilla et al., 2017) or fault zones (Bodvarsson et al., 1997; Liu et al., 2004) may lead to the formation of preferential flow paths in the vadose zone triggering rapid mass fluxes
- The non-linear nature of free-surface flow and mass partitioning processes at fracture intersections may be difficult to recover by volume-effective modelling approaches (e.g. Richards' equation) and unified conceptual frameworks do not exist (Ghezzehei, 2004)

2. Analogue experiments

- Well controlled analogue percolation experiments may aid to investigate the formation of flow modes and instabilities (Jones et al., 2018; Li et al., 2018) and the role of unsaturated fracture intersections on mass partitioning processes (e.g., Ji et al., 2006; Kordilla et al., 2017; LaViolette et al., 2003; Nicholl and Glass, 2005; Wood et al., 2002, 2005; Wood and Huang, 2015)
- These studies highlight the importance of fracture intersections as capillary barriers, which may induce pulsating flows and act as integrators for dispersion and recharge processes

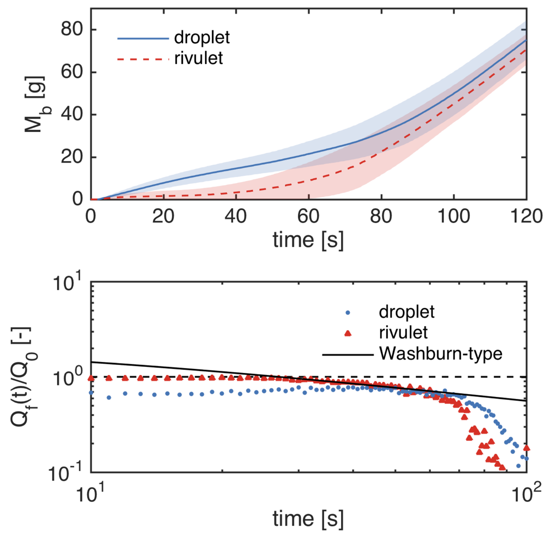

Figure 1: Accumulated mass M_b (top) and normalized fracture inflow rates (bottom) vs. time in analogue percolation experiments (after Kordilla et al., 2017).

3. Objective

- Confirm strong contrast in the bypass efficiency of droplet and rivulet flow observed in former experiments (Kordilla et al., 2017)
- Test an analytical solution for capillary-driven fracture inflow proposed by Kordilla et al. (2017)
- Apply a transfer-function approach for predictive modelling of mass partitioning processes at unsaturated fracture intersections of arbitrary-sized fracture cascades (Jury, 1986; Noffz et al., 2018)

II. Methods

1. Experimental approach

- The analogue fracture network consists of two to four vertically stacked poly(methyl methacrylate) (PMMA) cubes (20 cm × 20 cm × 20 cm)
- Aperture width d_f is either 1 mm or 2.5 mm
- The non-porous substrate exhibits a static contact angle θ_0 of $65.2 \pm 2.9°$
- Two injection methods are tested while the total volumetric flow rate Q_0 is 15 ml min^{-1}:

❶ 15×1 ml min^{-1} (droplet flow)

❷ 3×5 ml min^{-1} (rivulet flow)

Figure 2: Injection methods used in analogue percolation experiments.

II. Methods (cont.)

2. Mass partitioning

- The total injected mass M at time t is

$$M(t) = Q_0 t \tag{1}$$

- Its redistribution at the unsaturated fracture intersection is given by

$$M(t) = M_f(t) + M_1(t) \tag{2}$$

- Here, M_f is the mass in the fracture and M_1 the mass accumulated on the drip pan. Derivation of Eq. (2) gives

$$\frac{dM(t)}{dt} = Q_0 = \frac{dM_f(t)}{dt} + \frac{dM_1(t)}{dt} \tag{3}$$

- Hence, the volumetric fracture inflow rate Q_f $[L^3T^{-1}]$ is

$$Q_f(t) = \frac{dM_f(t)}{dt} = Q_0 - Q_1(t) \tag{4}$$

3. Washburn-type fracture inflow

- An analytical solution for capillary driven fracture inflow Q_f following Washburn (1921) and Bell & Cameron (1905) is proposed by Kordilla et al. (2017). Penetration length $l(t)$ is obtained by

$$\frac{dl(t)}{dt} = \frac{d_f^2 \Delta P_c}{4\eta\, l(t)} \tag{5}$$

- Here, η is viscosity and ΔP_c capillary pressure. For the initial length (i.e. $l(t = t_0) = l_0$) Eq. (5) gives

$$l(t) = l_0 \sqrt{1 + \frac{d_f^2 \Delta P_c}{2\eta l_0^2}(t - t_0)} \tag{6}$$

- The fluid mass within the fracture is $M_f(t) = A_f l(t) \rho_w$, where ρ_w accounts for water density and A_f for the cross-sectional fracture area

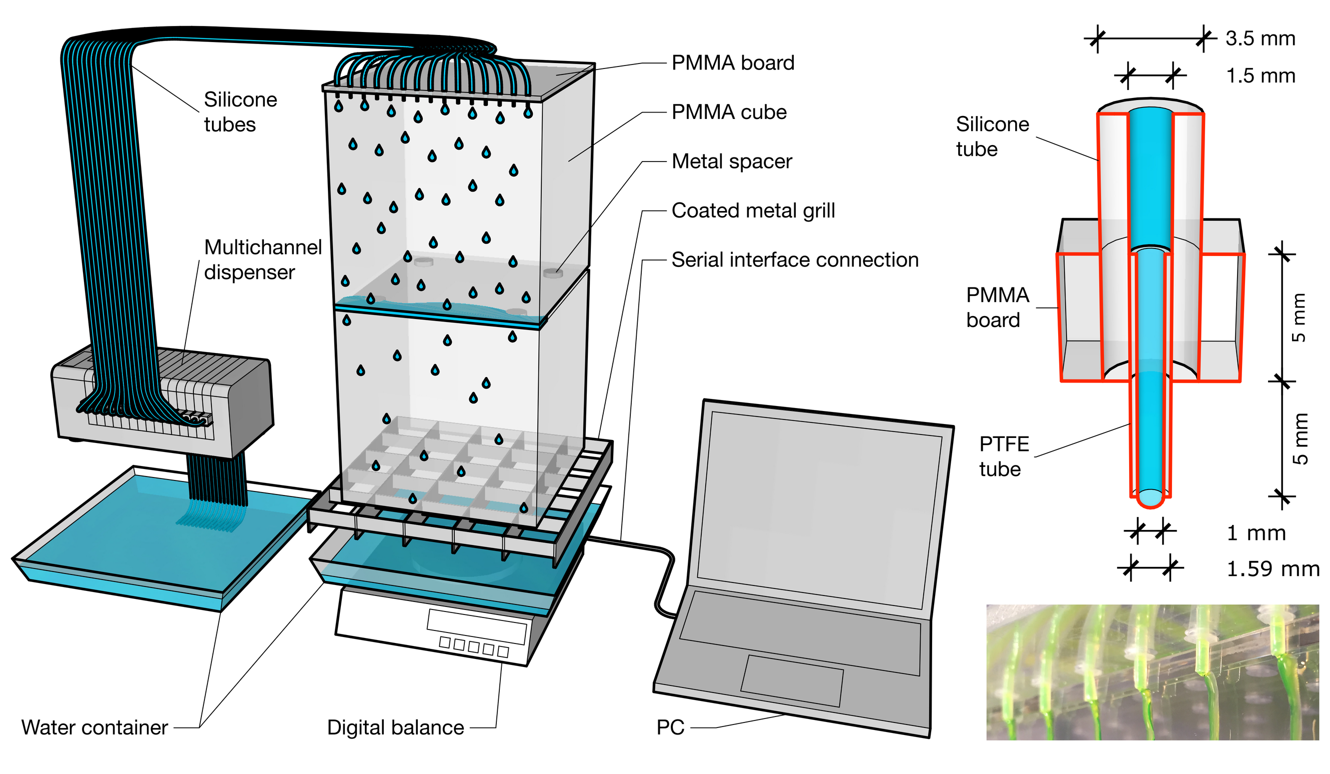

Figure 3: Sketch of laboratory setup (left) and injection nozzle (right). From Noffz et al. (2018).

- The flow rate into the fracture according to Eq. (4) becomes

$$Q_f(t) = \frac{Q_0}{\sqrt{1 + 2k_f(t - t_0)}} \tag{7}$$

- The transition constant is defined as $k_f = \frac{d_f^2 \Delta P_c}{2\eta l_0^2}$

4. Transfer function

- The outflow rate at the bottom of the network is considered in the context of transfer function theory (Jury, 1986)
- The output signal $Q_{n+1}(t)$ at the bottom of cube n is given in terms of the input signal $Q_n(t)$ at the top as

$$Q_{n_f}(t) = \int_0^t \varphi_{n_f}(t - t') Q_{n_f - 1}(t') \tag{8}$$

- Here, $\varphi_{n_f}(t)$ is the transfer function that accounts for vertical film flow and flow partitioning in cube n. For a single fracture the relation is

$$Q_1(t) = Q_0 \int_0^t dt' \varphi(t') \tag{9}$$

- The transfer function is characteristic of the mass redistribution at the fracture intersection and relates to the flow rate at the drip pan and within the fracture as

$$\varphi(t) = \frac{dQ_1(t)}{dt} = -\frac{dQ_f(t)}{dt} \tag{10}$$

- For rivulet flow the transfer function may be estimated from the output signal at the bottom of the second cube according to Eq. (10)
- The transfer function is zero before the onset of the Washburn type flow t_0 and reaches a maximum after which it decreases exponentially fast
- The truncated Gaussian is employed to capture these features

$$\varphi(t) \propto \frac{\exp\left[-\frac{(t-\mu)^2}{2\sigma^2}\right]}{\sqrt{2\pi\sigma^2}} \tag{11}$$

- Here, μ denotes the mean and σ^2 the variance
- Furthermore, the transfer function is normalized to 1, hence

$$\int_0^\infty dt \varphi(t) = 1 \tag{12}$$

- For the total fracture flow the approach gives Q_{f,n_f} after n_f cubes

$$Q_{f,n_f}(t) = Q_0 \ldots \tag{13}$$

$$\left[1 - \int_0^t dt_{n_f-1} \varphi(t - t_{n_f-1}) \ldots \int_0^{t_3} dt_2 \varphi(t_3 - t_2) \int_0^{t_2} dt_1 \varphi(t_1)\right]$$

III. Results & Discussion

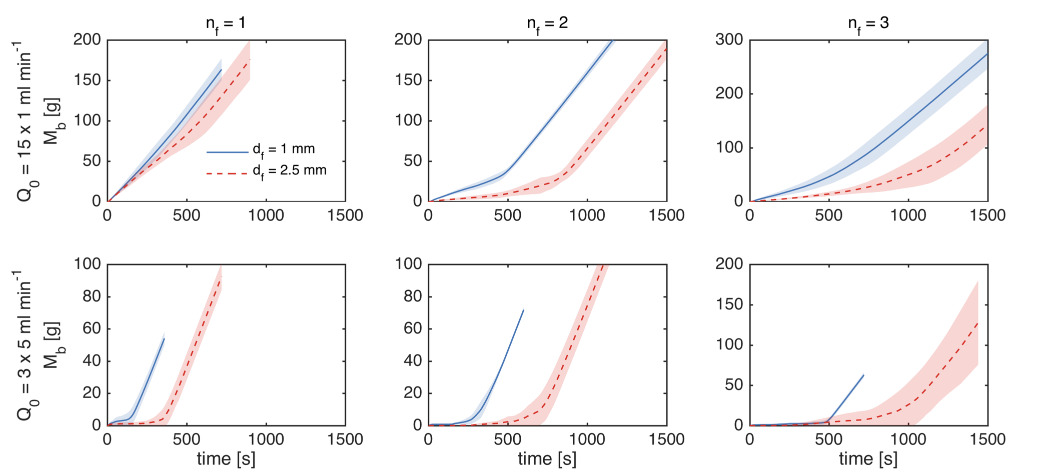

Figure 4: Accumulated mass M_b vs. time for droplet (top) and rivulet flow (bottom) produced by a multi-inlet array. From Noffz et al. (2018).

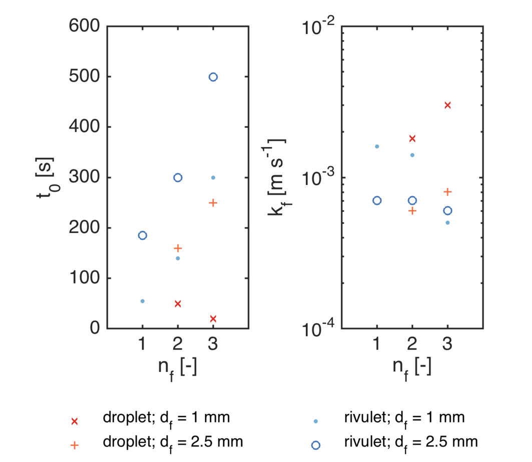

Figure 5: Adjusted parameters t_0 and k_f for fitting of Eq. (7). From Noffz et al. (2018).

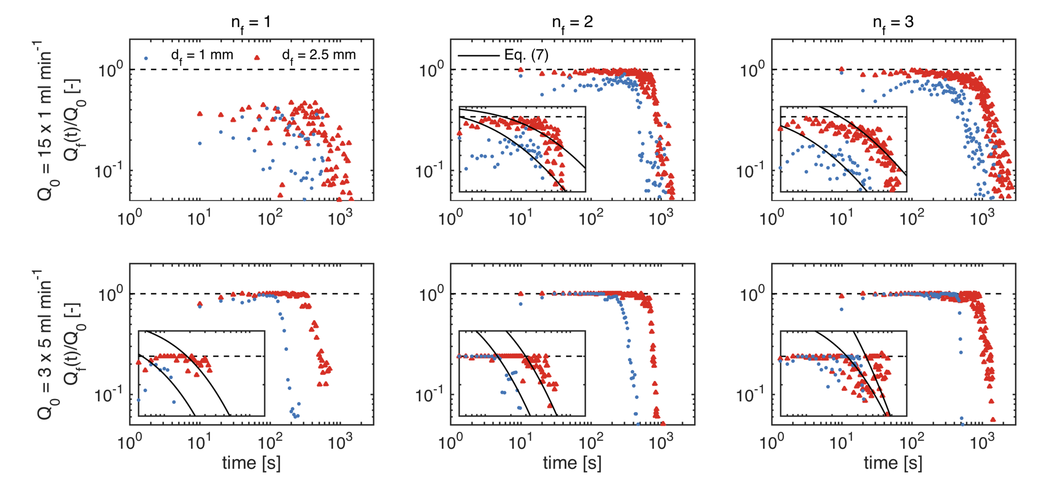

Figure 6: Normalized fracture inflow rate Q_f/Q_0 for multi-inlet experiments. Insets show fitted Eq. (7). From Noffz et al. (2018).

III. Results & Discussion (cont.)

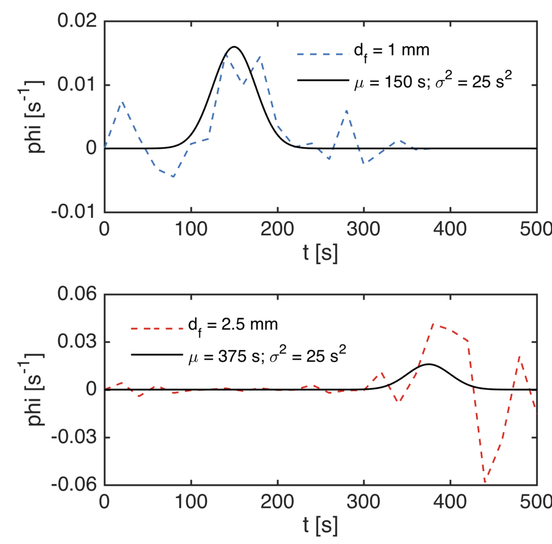

- Droplet flow exhibits a higher bypass efficiency than rivulet flow
- Transition into a Washburn-type flow regime is recovered by an analytical solution for capillary-driven fracture inflow
- Gaussian transfer function reproduces main characteristics of the mass partitioning process during rivulet flow and shows good agreement with experimental data for $1 \le n_f \le 3$

Figure 7: Transfer functions φ for rivulet flow at a single fracture intersection (dashed lines) and fitted Gaussian (solid lines). From Noffz et al. (2018).

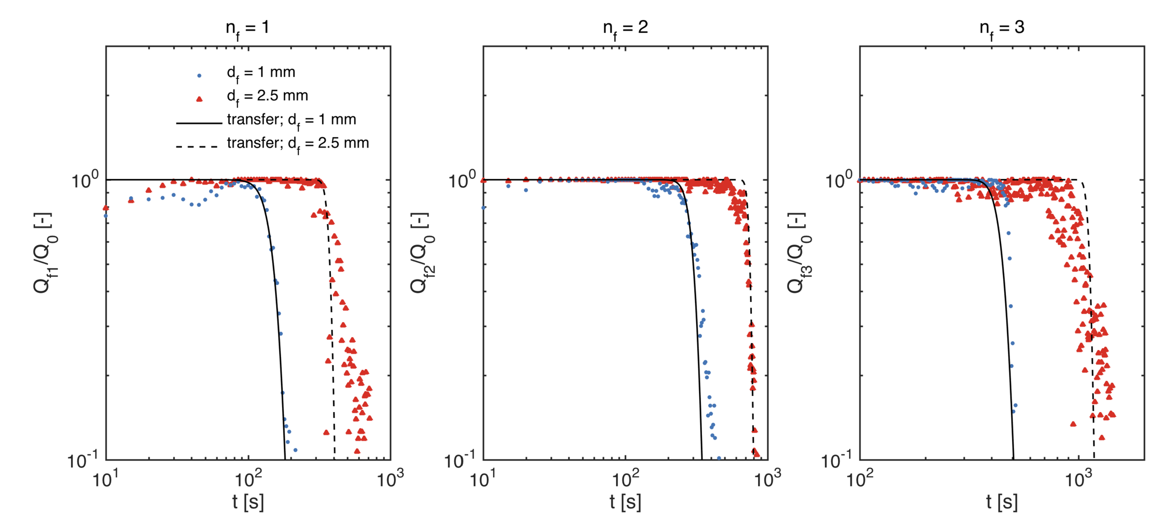

Figure 8: Normalized fracture inflow rates Q_f/Q_0 during rivulet flow with predictions obtained by Eq. (13). From Noffz et al. (2018).

IV. Conclusion

1. Mass redistribution at unsaturated fracture intersections

- A high bypass efficiency of droplet flow and the existence of a Washburn-type flow regime have been successfully presented in analogue percolation experiments
- The transfer function approach enables predictive modelling of mass partitioning dynamics during rivulet flow for arbitrary-sized fracture cascades (i.e. $n_f \ge 1$)

2. Limitations

- Tested fracture geometries are highly simplified and chosen materials do not account for the imbibition of a porous matrix

3. Outlook

- Further studies are required to investigate the impact of geometric features of natural fracture systems (e.g., roughness, aperture width, inclination) and material properties (e.g., wetting, contact angle dynamics, matrix-fracture interaction)

Acknowledgements:
This work was funded by the Deutsche Forschungsgemeinschaft (DFG; German Research Foundation) under grant no. SA 501/26-1 and KO 53591/1-1. Marco Dentz acknowledges the funding from the European Research Council under the European Union's Seventh Framework Programme (FP7/2007-2013)/ ERC Grant Agreement No. 617511 (MHetScale).

References:
Bell et al. (1905): J. of Phys. Chem. **(10)**; Bodvarsson et al. (1997): Earth Sci. Div.; Dahan et al. (1999): Water Resour. Res. **(35)**; Dahan et al. (2000): Groundwater **(38)**; Ghezzehei (2004): Water Resour. Res. **(40)**; Ji et al. (2006): Water Resour. Res. **(42)**; Jones et al. (2018): Hydrogeol. J. **(26)**; Jury (1986): Water Resour. Res. **(22)**; Kordilla et al. (2017): Water Resour. Res. **(53)**; LaViolette et al. (2003): Geophys. Res. L. **(30)**; Li et al. (2018): Energies **(11)**; Liu et al. (2004): J. of Cont. Hydrol. **(74)**; Nicholl et al. (2005): Vad. Zone J. **(4)**; Nimmo (2012): Hydr. Proc. **(26)**; Noffz et al. (2018): Vad. Zone J.; Washburn (1921): Phys. Rev. **(15)**; Wood et al. (2002): Geophys. Res. L. **(29)**; Wood et al. (2005): Water Resour. Res. **(41)**; Wood et al. (2015): Fl. Dyn. in Compl. Fract. Por. Sys.